Alternative Pathways for Radical Dissipation in an Active Site Mutant of B_{12}-Dependent Methylmalonyl-CoA Mutase†

Dominique Padovani and Ruma Banerjee*

Redox Biology Center and Biochemistry Department, University of Nebraska, Lincoln, Nebraska 68588-0664

Received August 29, 2005; Revised Manuscript Received November 29, 2005

ABSTRACT: Methylmalonyl-CoA mutase catalyzes the adenosylcobalamin-dependent rearrangement of (2*R*)-methylmalonyl-CoA to succinyl-CoA. The crystal structure of the enzyme reveals that Y243 is in van der Waals contact with the methyl group of the substrate and suggests a possible role for it in the stereochemical control of the reaction. This hypothesis was tested by designing a molecular hole by replacing the phenolic side chain of Y243 with the methyl group of alanine. The Y243A mutation lowered the catalytic efficiency $>(4 \times 10^4)$-fold compared to wild-type enzyme, the $K_{M_{app}}$ for the cofactor ∼4-fold, and the cob(II)alamin concentration under steady-state turnover conditions ∼2-fold. However, the mutation did not appear to lead to loss of the stereochemical preference for the substrate. The Y243A mutation is expected to create a cavity and should, in principle, allow accommodation of bulkier substrates. To test this, we used ethylmalonyl-CoA and allylmalonyl-CoA as alternate substrates. Surprisingly, both analogues resulted in suicidal inactivation, albeit in an O_2-dependent and O_2-independent fashion, respectively. The inactivation by allylmalonyl-CoA was further investigated, and revealed formation of cob(II)alamin at an ∼1.5-fold higher rate than with wild-type mutase under single-turnover conditions. Product analysis revealed a stoichiometric mixture of 5′-deoxyadenosine, aquocobalamin, and allylmalonyl-CoA. Taken together, these results are consistent with an internal electron transfer from cob(II)alamin to the substrate analogue radical. These studies serve to emphasize the fine control exerted by Y243 in the vicinity of the substrate to minimize radical extinction in side reactions.

Methylmalonyl-CoA mutase catalyzes the reversible isomerization of methylmalonyl-CoA to succinyl-CoA and is dependent on 5′-deoxyadenosylcobalamin (AdoCbl)[1] or coenzyme B_{12} for activity (Figure 1) (*1*). In this reaction, the AdoCbl cofactor is used as a radical reservoir that generates, via homolysis of the Co-carbon bond, a pair of radicals: cob(II)alamin and a reactive 5′-deoxyadenosyl radical (Ado•). The latter abstracts a hydrogen atom from the substrate, generating a substrate-centered radical, which, in turn, rearranges to a product-centered radical. The remainder of the catalytic cycle is completed by reversal of the sequence of steps in the first half of the reaction (Figure 1).

Two questions of long-standing interest regarding AdoCbl-dependent enzymes are how the inherent kinetic inertness of the cobalt−carbon bond is overcome to effect a trillion-fold acceleration in the homolysis rate (*2*) and how the high reactivity of radical intermediates is controlled to minimize side reactions. Over the past decade, experimental and computational studies on methylmalonyl-CoA mutase have begun to provide insights into these issues (*3*−*8*). They point to the critical role played by individual active site residues in labilizing the cobalt−carbon bond (*7*) and in shielding radical intermediates from unwanted side reactions (*4*, *6*, *8*).

The crystal structure of methylmalonyl-CoA mutase from *Propionibacterium shermanii* reveals that the substrate reaches into the active site through a TIM-barrel positioned on the upper face of the corrin macrocycle (*9*). A ring of aromatic residues that include Y89, Y243, and H244 form a collar around the substrate (Figure 2). In addition, R207 makes electrostatic contacts with the carboxylate group of the substrate. We have been investigating the contributions to catalysis of individual active site residues in the immediate proximity of the substrate by assessing the properties of site-specific mutants.

In agreement with high-level ab initio calculations that predicted a role for partial protonation of substrate by H244 in reducing the energy barrier for rearrangement (*10*), mutation of this residue leads to loss of one of two titrable pK_a's that govern activity and a $>10^2$-fold decrease in the k_{cat} compared to wild-type enzyme (*4*). These studies also revealed that H244 plays a major role in shielding the active site from oxygen (*4*, *6*). The hypothesis that Y89 functions as a molecular wedge that labilizes the cobalt−carbon bond was derived from crystallographic data, which revealed that substrate-driven barrel closure results in a large motion of this residue and steric crowding above the corrin ring (*9*, *11*). The role of Y89 in labilizing the cobalt−carbon bond was supported by mutagenesis and kinetic studies, which also revealed its contribution to the rearrangement step (*3*, *7*).

† This work was supported by grants from the National Institutes of Health (DK45776 and P20RR17675, which supports the Spectroscopy and Mass Spectrometry Facilities of the Redox Biology Center).

* Corresponding author. E-mail: rbanerjee1@unl.edu. Telephone: (402)-472-2941. Fax: (402)-472-4961.

[1] Abbreviations: AdoCbl, 5′-deoxyadenosylcobalamin; MeCbl, methylcobalamin; Ado•, 5′-deoxyadenosyl radical; CoA, coenzyme A; TFA, trifluoracetic acid; H_2OCbl, aquocobalamin.

10.1021/bi051742d CCC: $33.50
Published on Web 02/10/2006

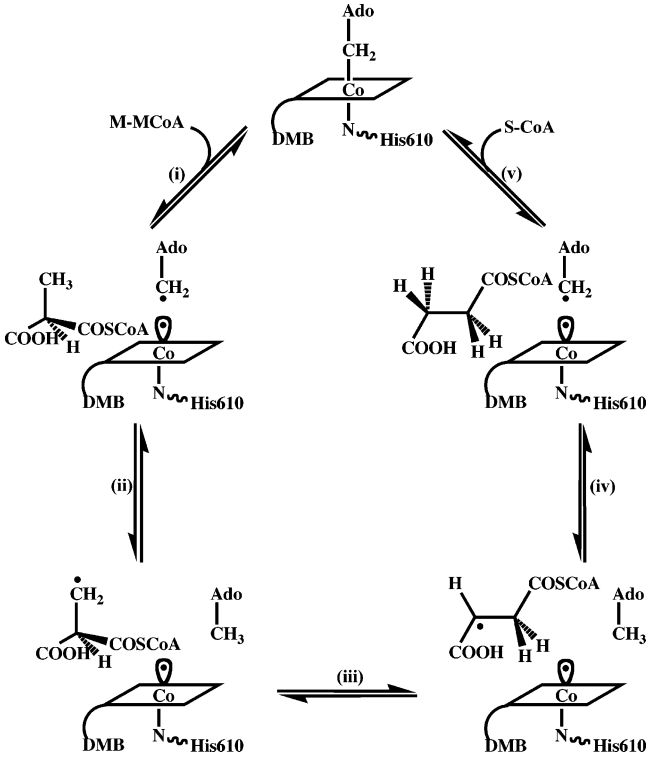

FIGURE 1: Postulated reaction mechanism for methylmalonyl-CoA mutase. M-MCoA and S-CoA denote methylmalonyl-CoA and succinyl-CoA, respectively.

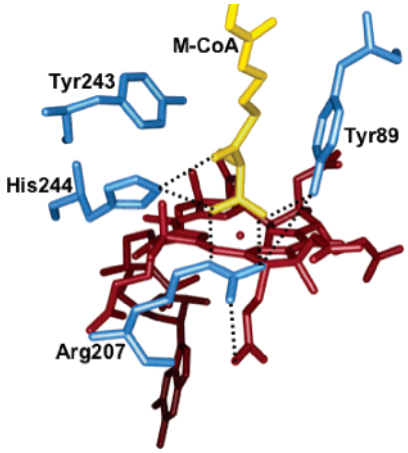

FIGURE 2: Close-up of the active site of methylmalonyl-CoA mutase. In this representation, the product of the reaction, succinyl-CoA (in yellow), enters through an aromatic corridor composed of H244, Y89, and Y243 (in blue). The B_{12} is shown in red. The structure was generated from the PDB file 4REQ.

It has been proposed that during the radical rearrangement, the methylene group in the product radical must flip from one side of the active site to the other to achieve the observed stereochemical outcome of the rearrangement reaction, that is, retention (*12*). It is attractive to consider the aromatic corridor, and in particular Y243, as a facilitator of this movement that guides the stereochemical route of the isomerization reaction. The crystal structure of methylmalonyl-CoA mutase reveals that Y243 is in van der Waals contact with the methyl group of the substrate (Figure 2) and could be positioned to help exert stereochemical control over the rearrangement reaction. To test this hypothesis, we have examined the effect of mutating Y243 to alanine, thereby creating a molecular cavity in the active site abutting the methyl group of the substrate. The Y243A mutation has multiple small effects on the steady-state kinetic properties of the enzyme but does not appear to lead to loss in the stereochemical preference for the substrate. The mutation results in enhanced susceptibility of the enzyme to suicidal inactivation in both an oxygen-dependent and an oxygen-independent fashion. These results emphasize the fine control exerted by each active site residue in the vicinity of the substrate for ensuring the fidelity of the reaction catalyzed by the native enzyme and in protecting radical intermediates from being quenched by internal electron transfer to the substrate/product radical.

EXPERIMENTAL PROCEDURES

Materials. AdoCbl and MeCbl were purchased from Sigma. Allylmalonic acid was purchased from Fluka; ethylmalonic acid and methylmalonic acid were purchased from Aldrich. [^{14}C]-CH_3-malonyl-CoA (56 Ci/mol) was purchased from New England Nuclear. All other chemicals were reagent grade and were used without further purification.

Construction of Site-Specific Mutant. The plasmid vector pKOS116-95b containing the *Propionibacterium shermanii* mutase gene (*13*) was a generous gift from Kosan Bioscience. The site-directed mutant was created using the QuickChange kit (Stratagene) and the following sense primer: 5′-GATTTCCATTTCCGGCGCCCACATGCAGGAAGC-3′. The mutagenic codon specifying alanine is underlined. The antisense mutagenic primer had the complementary sequence. Following PCR amplification, a 1.9-kb *Fse*I−*Hin*dIII fragment containing the mutation was excised and ligated into pKOS116-95b digested with the same restriction enzymes. The entire 1.9-kb fragment was sequenced at the Genomics Core Facility (University of Nebraska, Lincoln) in the forward and reverse directions to confirm the presence of the Y243A mutation.

Enzyme Expression and Purification. The wild-type and mutant apoenzymes were purified using a modification of the published procedure (*14*). The *Escherichia coli* strain, BL21(DE3), freshly transformed with the pKOS plasmid (encoding wild-type or the Y243A mutant of methylmalonyl-CoA mutase) was used to directly innoculate Luria broth medium (100 μL transformed cells per liter of culture) supplemented with 100 μg/mL carbenicillin. The cultures were grown overnight (~12 h) at 37 °C to an OD_{600} of 0.5 and induced at 27 °C with 0.5 mM IPTG and grown for an additional 6−8 h. Cells were harvested and disrupted by sonication, and the enzyme was purified essentially as described previously (*14*), except that the phenyl-Sepharose column was omitted. Instead, mutase-containing fractions pooled after the Q-Sepharose column were concentrated, washed extensively with 50 mM potassium phosphate buffer, pH 7.5, and directly loaded on to a 3 cm × 40 cm Matrix-Blue Dextran column, which was eluted as described (*14*). Protein concentration was determined using the Bradford reagent (BioRad) with bovine serum albumin as a standard.

Enzyme Assays. The specific activity of methylmalonyl-CoA mutase was determined in the radiolabeled assay at 37 °C as described previously (*15*). One unit of activity corresponds to the formation of 1 μmol of succinyl-CoA per minute. The kinetic parameters for the mutant were determined by increasing the duration of the assay from 3 to 10

min in the presence of 25 mM (*R*,*S*)-[^{14}C]-methylmalonyl-CoA. The kinetic parameters for the wild-type enzyme were determined in the presence of varying concentrations of (*R*,*S*)-[^{14}C]-methylmalonyl-CoA (50−2000 μM). The concentration of AdoCbl was kept constant in these assays and was at least 10-fold higher than the apoenzyme concentration.

Determination of Equilibrium Binding Constants for AdoCbl by Fluorescence Spectroscopy. Addition of the cofactor to the apomutase results in a decrease in fluorescence emission at 340 nm and was used to determine the equilibrium dissociation constant for AdoCbl as described previously (*16*). The enzyme concentration (wild-type or mutant) used in these experiments was 0.4 μM in 50 mM potassium phosphate buffer, pH 7.5. Successive aliquots (1−4 μL) of a 50 μM stock of AdoCbl solution prepared in the same buffer were added followed by incubation at 4 °C for 30 min prior to measurement of the fluorescence emission, and the data were analyzed as described previously (*16*).

Determination of the Equilibrium Binding Constant for AdoCbl by UV−Visible Absorption Spectroscopy. Binding of AdoCbl to the mutase was followed spectrophotometrically as previously described (*16*). The enzyme concentration used in these experiments was 25 μM, and the final AdoCbl concentration was varied from 1.5 to 60 μM. The K_d values were obtained by analyzing the data as described (*16*).

Determination of the Equilibrium Binding Constant for Methylmalonyl-CoA by UV−Visible Absorption Spectroscopy. Binding of methylmalonyl-CoA to the mutase reconstituted with MeCbl results in a blue shift in the α,β bands (*17*) and provides a convenient monitor for binding since the substrate does not turnover under these conditions. The titration was performed as follows. Apomutase (wild-type or mutant, 30 μM) in 200 μL of 50 mM potassium phosphate buffer, pH 7.5, was used as a blank. The enzyme was then reconstituted with MeCbl, and excess cofactor was removed by centrifugation using a Microcon YM30 membrane (Millipore). Spectra of MeCbl-reconstituted holomutase were recorded between 750 and 300 nm after each addition of methylmalonyl-CoA (3 μL aliquots of a 1.4 mM solution for the wild-type and 1.5 μL aliquots of a 140 mM solution for the mutant), following incubation at 4 °C for 20 min. The values for $\Delta A_{522\ nm}$ were plotted versus the concentration of methylmalonyl-CoA, and the K_d was determined by fitting the data to a modified Michaelis−Menten equation (eq 1), where *S* is the concentration of methylmalonyl-CoA.

$$\Delta A = \Delta A_{max} S/(K_d + S) \quad (1)$$

Purification and Assay of Malonyl-CoA Synthetase. The plasmid vector, pKII, containing the *Rhizobium trifolii* malonyl-CoA synthetase gene inserted between two 6-His Tag cassettes was a gift from Prof. Chaitan Khosla (Stanford University). *E. coli* BL21(DE3) cells transformed with the pKII plasmid were grown to an OD_{600} of 0.5 at 37 °C in Luria broth supplemented with 100 mg/L ampicillin. The temperature was then switched to 22 °C, and the culture was induced with 0.5 mM IPTG when the OD_{600} was ∼1.0 and grown for an additional 24 h. Cells were harvested and resuspended in lysis buffer (50 mM sodium phosphate buffer, pH 8.0, 300 mM NaCl, 10 mM imidazole, 0.1 mM PMSF, and 0.25 mg/mL lysozyme). The mixture was stirred at 4 °C for 60 min; then the cells were disrupted by sonication. After centrifugation, the supernatant was filtered through a 0.2 μm syringe filter (Nalgene) and loaded on a Ni-NTA column (1 cm × 5 cm). Prior to elution, the column was washed with 10 volumes of 50 mM sodium phosphate buffer, pH 8.0, containing 300 mM NaCl and 10 mM imidazole. The enzyme eluted from the column with ∼100 mM imidazole in 50 mM sodium phosphate buffer, pH 8.0 containing 300 mM NaCl. Pooled fractions were washed with 100 mM potassium phosphate buffer, pH 7.0, and stored on ice.

The activity of malonyl-CoA synthetase was estimated as follows using methylmalonic acid as a substrate. The assay mixture (1 mL total volume in 100 mM potassium phosphate buffer, pH 7.0) containing 40 mM methylmalonic acid, 20 mM $MgCl_2$, 5 mM ATP, and 5−10 μg of malonyl-CoA synthetase was employed as a blank. The reaction was started by adding 0.5 mM CoA and was monitored spectrophotometrically at 232 nm for 15 min at 20 °C. The activity of malonyl-CoA synthetase was determined by plotting $A_{232\ nm}$ (formation of the product thioester bond) versus time and by fitting the initial velocity data to a linear function. The specific activity of malonyl-CoA was estimated using eq 2 (*18*), where *k* is the rate constant previously determined, $\epsilon_{232\ nm}$ is the extinction coefficient for methylmalonyl-CoA (10 mM^{-1} cm^{-1}), and *C* is the amount in milligrams of malonyl-CoA synthetase used in the assay.

$$SA = k/(\epsilon_{232\ nm} C) \quad (2)$$

Purified malonyl-CoA synthetase had a specific activity of ∼1.4 μmol min^{-1} mg^{-1} at 20 °C.

Enzymatic Synthesis and Purification of Methyl-, Ethyl-, and Allylmalonyl-CoA. The reaction mixture (20 mL total volume), containing 20 mM methyl-, ethyl-, or allylmalonic acid, 20 mM $MgCl_2$, 3 mM ATP, 2 mM CoASH, and 6 mg of malonyl-CoA synthetase, was prepared in a reaction buffer containing 100 mM potassium phosphate buffer, pH 7.0. After incubation for 6 h at room temperature, the solution was treated with TFA (1% final concentration) and centrifuged to remove the precipitated protein. The synthesized substrates were then filtered and purified by HPLC using a C_{18} reversed phase column with a gradient ranging from 0% to 40% acetonitrile in 0.1% TFA over 45 min at a flow rate of 5 mL min^{-1}, and the eluant was monitored at 254 nm. Under these conditions, methylmalonyl-CoA, ethylmalonyl-CoA, and allylmalonyl-CoA eluted at ∼12.2%, 17.1%, and 30.5%, acetonitrile, respectively. The fractions of interest were pooled and dried by lyophilization.

UV−Visible Absorption Spectroscopy of Enzyme−Substrate (Analogue) Complexes. To 20−30 μM holoenzyme in 50 mM potassium phosphate, pH 7.5, a solution of methylmalonyl-CoA (final concentration of 4−15 mM), ethylmalonyl-CoA (1 equiv), or allylmalonyl-CoA (1 equiv) was added. The same experiments were also carried out under strictly anaerobic conditions by purging the sealed cuvette with oxygen-free argon and adding an anaerobic solution of methylmalonyl-CoA (final concentration of 6 mM), ethylmalonyl-CoA (1−100 equiv), or allylmalonyl-CoA (1 equiv).

To determine the K_i for ethylmalonyl-CoA, 7 μM holoenzyme in 50 mM potassium phosphate buffer, pH 7.5, was mixed with various concentrations of ethylmalonyl-CoA (5,

10, 15, 20, 25, 50, and 75 μM final concentration) in the dark at 20 °C. The inactivation reaction was monitored by the rate of formation of H_2OCbl at 351 nm. Analysis of the dependence of k_{obs} on the concentration of ethylmalonyl-CoA yielded the values for K_i and the substrate-independent rate constant for inactivation (k_{inact}).

The kinetic parameters for inactivation by allylmalonyl-CoA were obtained by UV−visible stopped-flow spectrophotometry by monitoring the formation of cob(II)alamin and H_2OCbl. Holo-Y243A (9 μM after mixing) was rapidly mixed with various concentrations of allylmalonyl-CoA (7, 14, 21, 30, 50, and 100 μM after mixing) in 50 mM potassium phosphate buffer, pH 7.5, at 20 °C. Cob(II)alamin formation was monitored by a decrease in absorbance at 525 nm over a 0.5 s period, and H_2OCbl formation was monitored by an increase at 351 nm over an 8 s period. The k_{obs} at each wavelength was plotted versus the concentration of allylmalonyl-CoA and yielded the parameters, K_i and the substrate-independent rate constant for inactivation (k_{inact}). Each data point was the average of at least three independent experiments.

Stereoselectivity of the Y243A Mutant-Catalyzed Reaction. A change in the stereochemical selectivity of the Y243A mutase-catalyzed reaction was determined by following the consumption of (*R,S*)-methylmalonyl-CoA as a function of time. Typically, the mutant holomutase (30−50 μM) was incubated in the dark at 37 °C with 1−5 mM (*R,S*)-methylmalonyl-CoA in a total volume of 1 mL of 50 mM potassium phosphate buffer, pH 7.5. At various times ranging from 30 min to 12 h, 100 μL aliquots were removed and quenched with 10 μL of 1 M perchloric acid, incubated on ice for 10 min, and centrifuged. The supernatant was then analyzed by HPLC using a LunaC_{18} reversed phase column (250 mm × 4.6 mm, Phenomenex) with a gradient ranging from 0% to 40% acetonitrile in 0.1% TFA over 45 min at a flow rate of 1 mL min^{-1}, and the eluant was monitored at 254 nm. Under these conditions, methylmalonyl-CoA eluted at ∼12.2% acetonitrile. Control reactions were performed in which either apoenzyme or methylmalonyl-CoA was omitted from the reaction mixture.

HPLC Characterization of Inactivation Products during Reaction of Y243A with Allylmalonyl-CoA. A solution of 70 μM holoenzyme was mixed in the dark at 20 °C with 70 μM allylmalonyl-CoA in a total volume of 200 μL of 50 mM KPi, pH 7.5. After 30 min incubation, the reaction was digested with 5 μL of proteinase K (Ambion) for 4 h at room temperature and then quenched with 1 M perchloric acid (10% v/v), incubated on ice for 10 min, and centrifuged. The inactivation products formed were filtered through a 0.2 μm syringe filter (Nalgene) and monitored by HPLC using a LunaC_{18} reversed phase column (250 mm × 4.6 mm, Phenomenex) with a gradient ranging from 0% to 40% acetonitrile in 0.1% TFA over 45 min at a flow rate of 1 mL min^{-1}, and the eluant was monitored at 254 and 350 nm. Under these conditions, 5′-deoxyadenosine, OH_2Cbl, and allylmalonyl-CoA eluted at ∼14.9%, 20.7%, and 30.5% acetonitrile, respectively. Control reactions were performed in which either apoenzyme or allylmalonyl-CoA was omitted from the reaction mixture (AdoCbl at 70 μM concentration was added to the control lacking apoenzyme). 5′-Deoxyadenosine was purified by HPLC on a C_{18} reversed phase column using the method described above. Fractions were pooled and dried by lyophilization and further characterized by ESI-MS in a positive ion mode.

Stopped-Flow UV−Visible Spectroscopy. The inactivation kinetics with allylmalonyl-CoA and single-turnover experiments were carried out in an Applied Photophysics spectrophotometer (ISX.MV18) under red light illumination. Solutions of holomutase (50−60 μM of wild-type or mutant before mixing) in 50 mM potassium phosphate buffer, pH 7.5, and allylmalonyl-CoA (50−60 μM before mixing) in the same buffer were employed. For single-turnover experiments with the natural substrate, solutions of holomutase (90−100 μM wild-type before mixing) in 50 mM potassium phosphate buffer, pH 7.5, and (*R,S*)-methylmalonyl-CoA (180−200 μM before mixing) in the same buffer were employed. All solutions were filtered through a 0.2 μm syringe filter (Nalgene) and then transferred to the loading syringes and allowed to equilibrate for at least 20 min before initiating the experiments. An external water bath was used to maintain the loading syringes and the mixing chamber at 20 ± 0.5 °C. The concentration of holomutase was determined spectrophotometrically ($\epsilon_{525\ nm}$ = 9.06 mM^{-1} cm^{-1}). Following mixing, the reaction was monitored by a decrease in absorbance at 525 nm ($\Delta\epsilon_{525\ nm}$ = −4.8 mM^{-1} cm^{-1}, *15*) or an increase in absorption at 351 nm ($\Delta\epsilon_{351\ nm}$ = 15.06 mM^{-1} cm^{-1}). The reported rate constants represent the average of at least six independent experiments.

EPR Spectroscopy. X-band EPR spectra were recorded on a Bruker ESP300E spectrometer equipped with an Oxford ITC4 temperature controller connected to a Hewlett-Packard microwave frequency counter, model 5253B, and a Bruker gaussmeter, model ER 035. Samples were maintained in a Dewar filled with liquid helium inside the EPR X-band cavity. The specific conditions are given in the figure legends. The microwave power dependence of the EPR signals was determined at 10 and 25 K, and the value of the power for half saturation ($P_{1/2}$) was calculated by fitting the data to eq 3,

$$\log P = \log[(h/P^{1/2})/(h_0/P_0^{1/2})] \quad (3)$$

where the parameter h is the normalized EPR derivative signal amplitude obtained with microwave power P, and h_0 and P_0 are the corresponding quantities under nonsaturating conditions (*19*).

RESULTS

Steady-State Kinetic Properties of the Y243A Variant. The Y243A mutation does not affect the expression level or the chromatographic behavior of the resulting protein versus the wild-type enzyme, indicating that it does not cause gross structural perturbations. In contrast, comparison of the steady-state kinetic parameters (Table 1) reveals significant differences: the k_{cat} for formation of succinyl-CoA is diminished ∼500-fold, the K_M for methylmalonyl-CoA increased >450-fold, and the $K_{M_{app}}$ for AdoCbl decreased ∼4-fold. Thus, the Y243A mutant displays a >(2×10^5)-fold lower catalytic efficiency compared to the wild-type enzyme. The basis for the increased affinity for AdoCbl, albeit small, is not known.

The stereochemical preference of the enzyme is apparently unaffected by the Y243A mutation. As with wild-type enzyme, consumption of (*R,S*)-methylmalonyl-CoA by the Y243A ceases once ∼50% of the substrate is utilized (data

Table 1: Comparison of the Kinetic Parameters for Y243A and Wild-Type Enzyme

parameter	wild-type	Y243A
k_{cat},[a] s^{-1}	158	0.33
$K_{d-AdoCbl}$, nM	228 ± 28	56 ± 4
K_{MCoA},[b] μM	124 ± 7[a]	>10 000[a]
K_{D-MCoA}, μM	102 ± 22[c]	45 000 ± 11 000[c]
k_{cat}/K_M, M^{-1} s^{-1}	1.6 × 10^6	7.3
$[cob(II)alamin]_{s-s}$,[d] %	20	10
$K_{i-EMCoA}$,[a,b] μM	467 ± 26	15.3 ± 2.7[e]
$K_{i-AMCoA}$,[a,b] μM	425 ± 39	10.9 ± 1.1[e]

[a] Values obtained using the radiolabel assay at 37 °C. [b] MCoA, EMCoA, and AMCoA denote methylmalonyl-CoA, ethylmalonyl-CoA, and allylmalonyl-CoA respectively. [c] Values obtained by UV−visible spectroscopy at 20 °C. [d] $[Cob(II)alamin]_{s-s}$ refers to the concentration of cob(II)alamin under steady-state turnover conditions. [e] Values obtained by kinetic measurements at 20 °C as described under Experimental Procedures.

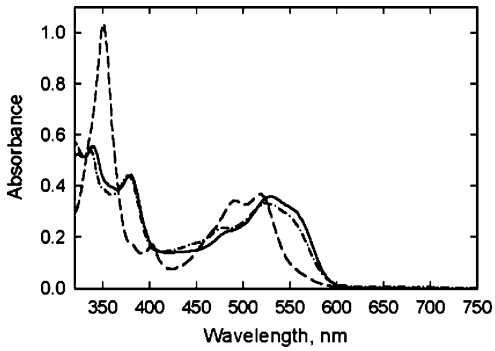

FIGURE 3: UV−visible spectra of the Y243A mutant in the presence of methylmalonyl-CoA or allylmalonyl-CoA. Enzyme (40 μM in 50 mM potassium phosphate buffer, pH 7.5, solid line) was incubated at 20 °C for 5 min with either methylmalonyl-CoA (20 mM, dashed−dotted line) or 1 equiv of allylmalonyl-CoA (dashed line).

not shown). The selectivity of the Y243A mutant was not determined and is presumed to be the same as that of the wild-type enzyme, that is, for the (*R*)-isomer.

Under steady-state turnover conditions, the wild-type enzyme contains a mixture of cob(II)alamin and AdoCbl in a ratio of ~1:4. With the Y243A mutant, cob(II)alamin accumulates to a lesser extent, and the ratio is reduced to ~1:9 (Figure 3) indicating a change in the magnitude of the relative energy barriers along the reaction coordinate.

Inactivation of Y243A by Substrate Analogues. The Y243A is expected to create a cavity in the active site and should, in principle, better accommodate bulkier substrate analogues. We tested two analogues with extended carbon skeletons: ethylmalonyl-CoA, a poor alternative substrate for wild-type enzyme (*20*, *21*), and allylmalonyl-CoA, which is predicted to stabilize the substrate allylic radical. With wild-type enzyme, both analogues act as competitive inhibitors and exhibit similar K_i values (~450 μM) (Table 1). The K_i values for the inhibitors are 30- to 40-fold lower for the mutant versus the wild-type enzyme, which is consistent with the improved accommodation of bulkier substrates in the cavity created in the mutant.

Addition of the substrate analogues does not elicit changes in the UV−visible spectrum of the wild-type enzyme (data not shown). In contrast, addition of 1 equiv of either ethylmalonyl-CoA or allylmalonyl-CoA to the Y243A mutant resulted in conversion of AdoCbl to H_2OCbl,

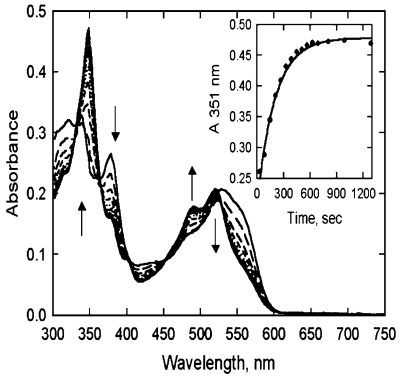

FIGURE 4: Ethylmalonyl-CoA-dependent formation of H_2OCbl in the Y243A mutant under aerobic conditions. Enzyme (25 μM in 50 mM potassium phosphate, pH 7.5, solid line) was incubated with 1 equiv of ethylmalonyl-CoA in the dark at 20 °C. The first spectrum was obtained after 30 s, and successive spectra were recorded every 45 s (dashed lines). The inset shows the time course for the formation of H_2OCbl monitored at 351 nm.

indicating inactivation (Figures 3 and 4). To distinguish between oxygen-dependent and oxygen-independent pathways for conversion of cob(II)alamin to H_2OCbl, the same reactions were monitored under strictly anaerobic conditions. Formation of H_2OCbl was observed with allylmalonyl-CoA but not with ethylmalonyl-CoA, even in the presence of a 100-fold excess of this analogue. This indicates that inactivation with ethylmalonyl-CoA likely involves interception of cob(II)alamin by oxygen, whereas with allylmalonyl-CoA, it involves an internal electron transfer. One of the products of inactivation, H_2OCbl, remains tightly bound to the enzyme and does not exchange with free AdoCbl (not shown). This is consistent with the inability of excess AdoCbl in the assay mixture to rescue inactivated enzyme.

Kinetics of Inactivation by Substrate Analogues. Inactivation in the presence of ethylmalonyl-CoA occurs with an isosbestic conversion of AdoCbl to H_2OCbl, which is consistent with the absence of detectable accumulation of intermediates (Figure 4). Formation of H_2OCbl was monitored at 351 nm and occurred with a k_{obs} of 0.3 ± 0.02 min^{-1} (Figure 4, inset) and a k_{inact} of ~0.40 ± 0.03 min^{-1}.

Inactivation of the Y243A mutant by allylmalonyl-CoA was monitored by stopped-flow spectroscopy. Transient formation of cob(II)alamin during inactivation by allylmalonyl-CoA was confirmed by multiple wavelength detection of spectral intermediates (Figure 5). Between $t = 0$ and 130 ms, allylmalonyl-CoA induces conversion of AdoCbl to cob(II)alamin with isosbestic points at 337, 387, and 484 nm (Figure 5, left panel). This is followed at t >130 ms by stoichiometric conversion of cob(II)alamin to H_2OCbl with isosbestic points at 335, 368, and 478 nm (Figure 5, right panel). The time course for the absorbance changes at 525 nm revealed biphasic kinetics (Figure 6). The first phase, corresponding to the formation of cob(II)alamin (Figure 5, right panel), is characterized by a rate constant of 35.5 ± 2.2 s^{-1} ($n = 6$) at 20 °C, which is similar to that estimated at 473 nm (36.2 ± 3.2 s^{-1}, $n = 5$), where the absorbance change is smaller (Figure 6, left panel). This corresponds to an ~1.5-fold higher rate of cobalt−carbon bond homolysis compared to the wild-type mutase in the presence of a stoichiometric amount of methylmalonyl-CoA (~26.6 ± 2.4 s^{-1} at 20 °C). On the basis of a $\Delta\epsilon = -4.8$ $mM^{-1}cm^{-1}$ (*15*), the change in absorbance at 525 nm between $t = 0$ and $t =$

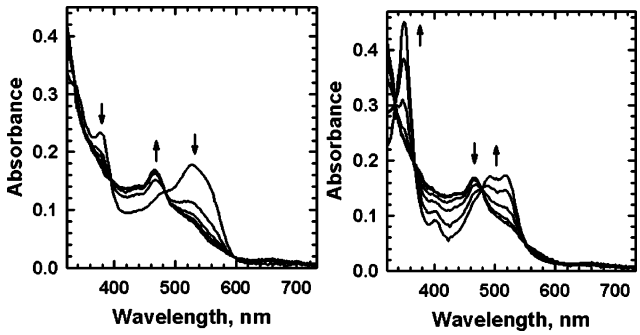

FIGURE 5: Spectral changes in Y243A induced by allylmalonyl-CoA under aerobic conditions. UV−visible absorption changes were monitored following rapid mixing of Y243A (24 μM final concentration) with 1 equiv of allylmalonyl-CoA at 20 °C. The spectra record changes between $t = 0$ and $t = 130$ ms (left panel) and between $t = 130$ ms and $t = 4.1$ s (right panel). The arrows indicate the direction of absorption changes.

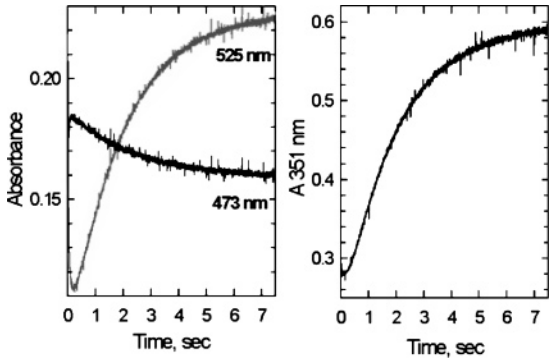

FIGURE 6: Kinetics of allylmalonyl-CoA-dependent inactivation of the Y243A enzyme. In the left panel, enzyme (25 μM final concentration) was rapidly mixed with 1 equiv of allylmalonyl-CoA, and changes in absorbance at 473 and 525 nm were recorded. In the right panel, the rate of H_2OCbl formation was monitored at 351 nm under analogous conditions.

130 ms indicates that ~90% of the enzyme exists as cob(II)alamin during this first phase. The second phase, corresponding to formation of H_2OCbl (Figure 5, right panel), is characterized by a rate constant of 0.54 ± 0.03 s^{-1}, $n = 3$ (monitored at 525 nm), which is similar to the value obtained at 351 nm (0.53 ± 0.02 s^{-1}, $n = 3$) (Figure 6, right panel). Based on a $\Delta\epsilon_{351\ nm} = 15.06$ mM^{-1} cm^{-1}, ~91% of the cofactor is in the H_2OCbl state indicating stoichiometric oxidation of cob(II)alamin. The kinetics of H_2OCbl formation were the same within experimental error under anaerobic conditions (not shown).

Characterization of the Inactivation Products with Allylmalonyl-CoA. The products of inactivation generated in the presence of allylmalonyl-CoA were separated by HPLC, and three peaks were observed. One with a retention time of 20.6 min was identified as 5′-deoxyadenosine based on its coelution with a standard, and its identity was confirmed by mass spectrometry (not shown). Two other peaks with retention times of 25.8 and 34.8 min, respectively, were assigned as H_2OCbl and allylmalonyl-CoA, respectively. However, the intensities of these peaks were weak and corresponded to 7.4% and 12.8% recovery, respectively, indicating that these compounds were released inefficiently during perchloric acid precipitation of the enzyme. This observation suggested the possibility that a covalent adduct could be formed between the substrate and the enzyme during the inactivation process.

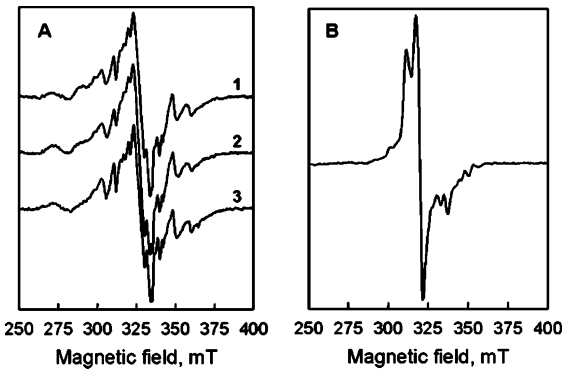

FIGURE 7: EPR spectra of the Y243A mutant. Panel A shows the spectrum of Y243A in the presence of methylmalonyl-CoA. Samples were prepared by mixing an aerobic solution of ice-cold apo-Y243A enzyme (250 μM final in 50 mM potassium phosphate buffer, pH 7.5) with 40 mM (final concentration) unlabeled methylmalonyl-CoA (spectrum 1), 2′-[CD_3]-methylmalonyl-CoA (spectrum 2) or [2,2′-D_4]-methylmalonyl-CoA (spectrum 3). The reaction was initiated by addition of 500 μM AdoCbl in the dark, mixed, and rapidly frozen by plunging the EPR tube into liquid N_2. The spectra were obtained by addition of 16 scans. Panel B shows the EPR spectrum of Y243A (86 μM final concentration of an aerobic sample in 50 mM potassium phosphate buffer, pH 7.5) rapidly mixed with 1 equiv of allylmalonyl-CoA. The spectra were acquired using the following conditions: modulation frequency, 100 kHz; modulation amplitude, 1 mT; power, 0.32 mW; gain, 10^5 in panel A and 10^4 in panel B; temperature, 25 K. The resonator frequency was 9.38 GHz.

To test this possibility, mass spectrometry was employed to assess the mass (80 014.91) of the large B_{12}-binding subunit in inactive enzyme, which was found to be identical to that in active enzyme (80 014.48), ruling out covalent modification. As an alternative to acid precipitation for releasing bound ligands, the inactivated enzyme was digested with proteinase K for 4 h at room temperature. Following this treatment, 5′-deoxyadenosine, H_2OCbl, and allylmalonyl-CoA were indeed recovered in an ~1:1:1 ratio as determined by HPLC analysis.

EPR Spectroscopy of Y243A. The existence of a biradical intermediate in the wild-type enzyme has been demonstrated by EPR spectroscopy, which reveals the presence of cob(II)alamin coupled to the succinyl-CoA radical (*22*). An EPR spectrum was observed when the mutant enzyme was mixed with protiated methylmalonyl-CoA and frozen rapidly that is broad and exhibits hyperfine splittings in the high field region that have a spacing of ~100 G (Figure 7, spectrum 1). The S-shaped signal has a crossover *g*-value of ~2.05 and exhibits a power for half-saturation, $P_{1/2}$, of 364 ± 7 μW at 10 K and 1.10 ± 0.03 mW at 25 K.

Perturbations of the EPR spectrum were not observed upon isotopic substitutions in the substrate. Thus, [2′-CD_3]-methylmalonyl-CoA or perdeuterated substrate generate spectra that are similar to that obtained with the protiated substrate (Figure 7A, spectra 2 and 3). The spectra resemble that observed with wild-type enzyme incubated with 2-carboxyethyl-CoA (*21*) and appear to represent cob(II)alamin that is not coupled to an organic radical.

The EPR spectrum of the biradical species observed in the presence of allylmalonyl-CoA is different (Figure 7B). The S-shape feature has a crossover *g* value of ~2.097, is less resolved, and resembles the spectrum obtained with the wild-type enzyme in the presence of the succinyl-dethia-

(dicarba)-CoA analogue (*23*). Hyperfine splittings (~50 G) are observed in the high field region and the signal exhibits a power for half-saturation $P_{1/2} = 50 \pm 4$ μW at 10 K and $P_{1/2} = 2.19 \pm 0.08$ mW at 25 K. Prolonged incubation of the sample at room temperature led to the disappearance of the EPR signal, consistent with it representing a transient intermediate. Unavailability of labeled substrate precursors precluded assignment of the organic radical using isotopic perturbations of the EPR spectrum. Based on chemical principles, it is possible that the signal represents cob(II)-alamin coupled to the allylic radical, which is expected to be the most stable.

DISCUSSION

Crystal structures of methylmalonyl-CoA mutase reveal that the substrate makes a snug fit in an active site corridor lined with aromatic residues and is engaged in multiple electrostatic interactions with the protein (Figure 2). Since the mutase catalyzes its reaction under aerobic conditions with high fidelity, it begs the question as to how the enzyme protects its highly reactive radical intermediates and what roles the individual active site residues play in modulating and reining in radical reactivity. Studies with site-directed mutants in the immediate vicinity of the substrate have begun to illuminate these issues. In this study, we have evaluated the effects of mutating Y243, a component of the aromatic active site collar around the substrate, which is in van der Waals contact with the methyl group of methylmalonyl-CoA (Figure 2). The location of Y243 also suggests a role in governing substrate stereoselectivity and in promoting cobalt−carbon bond homolysis.

However, the stereochemical preference of the mutase-catalyzed reaction is apparently unaffected by the Y243A mutation. Indeed, as with wild-type enzyme, consumption of (*R*,*S*)-methylmalonyl-CoA by the Y243A mutant ceases once 50% of the substrate is utilized (data not shown). The steady-state kinetic parameters reveal that loss of the aromatic side chain in the Y243A mutant has multiple small effects on catalysis, which combine to decrease catalytic efficiency $>4 \times 10^4$ relative to that of the wild-type enzyme (Table 1). The major effect is on $K_{M(M-CoA)}$, which increases >80-fold and could not be measured accurately. Furthermore, a 2-fold decrease in the steady-state concentration of cob(II)-alamin is observed in the mutant (Figure 3), indicating a change in the relative energy barriers that contribute to limiting the reaction rate. In the wild-type enzyme, ~80% of the cofactor is in the AdoCbl form and 20% in the cob-(II)alamin state during steady state, which, combined with other data, has been interpreted as evidence for product release being the rate-limiting step (*2*). The decreased accumulation of cob(II)alamin in the Y243A mutant could result from a lower rate of cob(II)alamin formation (i.e., cobalt−carbon bond homolysis), a lower rate of product release, or both. The rate of cobalt−carbon bond homolysis was studied with the substrate analogue allylmalonyl-CoA and found to be comparable to that of wild-type enzyme and the natural substrate (Figure 6). This suggests that the Y243A mutation likely affects a step following the initial homolytic cleavage reaction.

The EPR spectrum observed in the presence of substrate is different from that seen with the wild-type enzyme (*22*). The spectrum of the mutant is broader than that seen with the wild-type enzyme, and the spacing of the hyperfine lines is 100 G versus 50 G for wild-type enzyme. It is assigned on the basis of its features and insensitivity to isotopic substitution in the substrate to cob(II)alamin alone (Figure 7A).

Loss of the phenolic side chain in the Y243A mutant is expected to create a molecular hole that should, in principle, accommodate bulkier substrates. To test this hypothesis, we used two analogues, each with extended carbon skeletons, as potential alternate substrates. The first, ethylmalonyl-CoA, has an extra carbon compared to the natural substrate, exhibits an ~10 000-fold lower catalytic rate with wild-type enzyme (*20*), and gives rise to an EPR signal that is similar to that observed with methylmalonyl-CoA (*21*). The second, allylmalonyl-CoA, has two additional carbons and is expected to stabilize the allylic radical if it is a substrate for the initial hydrogen atom abstraction by dAdo$^\bullet$.

Surprisingly, the substrate analogues lead to irreversible inactivation of Y243A, and their K_i values are 30−40-fold lower than the corresponding values for wild-type enzyme (Figures 3 and 4 and Table 1). Spectra of the inactivated enzyme reveal accumulation of the cofactor in the oxidized H_2OCbl state. Susceptibility to oxidation has previously been observed when two other active site residues were mutated, H244 and R207, albeit via different mechanisms. Mutation of H244 increased susceptibility of the enzyme to oxygen-based interception of the cob(II)alamin intermediate and could be averted under anaerobic conditions (*4*, *6*). In contrast, oxidation of the R207Q mutant occurred in an oxygen-independent manner with the substrate analogues isobutyryl-CoA and butyryl-CoA (*8*). Labeling studies were consistent with a mechanism involving internal electron transfer from cob(II)alamin to the substrate radical.

Interestingly, both pathways for H_2OCbl generation are observed with the Y243A mutant. With ethylmalonyl-CoA, inactivation is only observed under aerobic conditions implicating oxygen in the oxidation of cob(II)alamin. H_2-OCbl is formed at a rate of 0.4 ± 0.03 min^{-1}, which is significantly faster than $k_{H_2OCbl} \approx 4.2 \times 10^{-3}$ min^{-1} observed for the H244A mutant (*6*). Thus, an ~100-fold difference in the susceptibility to oxygen-based inactivation is observed between mutations at the two active site residues, Y243 and H244.

In the presence of allylmalonyl-CoA, suicide inactivation occurs in an oxygen-independent process, that is, by an internal electron transfer. The EPR spectrum of the biradical intermediate is distinct from that observed with the substrate, methylmalonyl-CoA (Figure 7). Cobalt−carbon bond homolysis induced by allylmalonyl-CoA binding leads to accumulation of cob(II)alamin at a rate (35.5 ± 2.2 s^{-1}) that is ~1.5-fold higher than that observed in the wild-type enzyme with methylmalonyl-CoA under single-turnover conditions. This small but significant difference might be explained by the greater steric bulk of allylmalonyl-CoA, which may contribute to greater destabilization of the cobalt−carbon bond. Alternatively, the greater stability of the resulting allylic versus the methylmalonyl-CoA radical, could account for the slightly greater rate of cobalt−carbon bond homolysis in the mutant. Accumulation of cob(II)alamin is then followed by its stoichiometric oxidation to H_2OCbl (Figures 5 and 6). H_2OCbl is formed at a rate of $0.54 \pm$

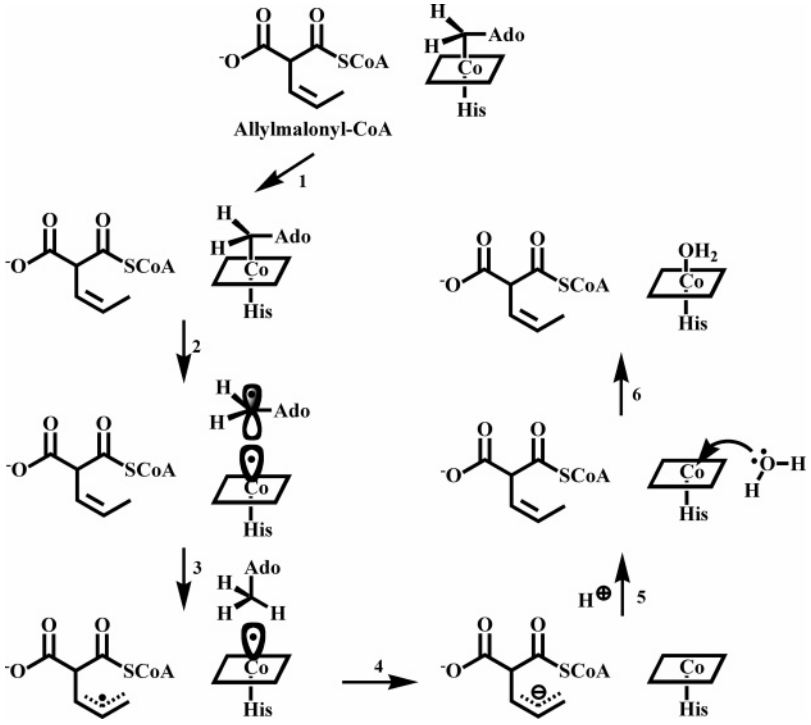

FIGURE 8: Proposed mechanism for the oxygen-independent suicidal inactivation of methylmalonyl-CoA mutase by allylmalonyl-CoA. The latter is arbitrarily depicted as being in the *Z*-conformation.

0.02 s^{-1}. Inactivation leads to recovery of allylmalonyl-CoA, H_2OCbl, and 5′-deoxyadenosine in a 1:1:1 ratio, which rules out covalent attachment between radical intermediates and the protein.

The proposed pathway for inactivation by allylmalonyl-CoA is described in Figure 8. Formation of the Michaelis−Menten complex is followed by cobalt−carbon bond homolysis, which generates cob(II)alamin and a highly reactive Ado•. The latter is predicted to abstract a hydrogen atom from allylmalonyl-CoA generating an allylic radical that is stabilized by resonance energy. The driving force for formation of an allylic radical would derive from the difference between the C−H bond dissociation energies in 5′-deoxyadenosine (100 kcal/mol) and in an allyl group (86 kcal/mol) (*24*) and the greater stability of the allylic radical relative to that of the 5′-deoxyadenosyl radical. Observation an EPR-active intermediate, tentatively identified as a biradical comprising cob(II)alamin coupled to the allylic radical (Figure 7B), is consistent with this pathway. It is likely that the stability of the allylic radical favors internal electron transfer from cob(II)alamin generating cob(III)alamin and a transient allyl anion ($pK_a \approx 45$ (*25*)). From a thermodynamic standpoint, this is an unfavorable electron transfer given the difference in the redox potential of the cob(III)alamin/cob(II)alamin ($E'° \approx +0.2$ V(*26*)) couple and the allyl anion/allyl radical ($E'° \approx -1.159$ V (*27*)) couple, which corresponds to a $\Delta G°$ of approximately +31.4 kcal/mol ($K \approx 4 \times 10^{-24}$ at 20 °C). However, once formed, the allyl anion would be protonated instantaneously in an exergonic reaction ($\Delta G° \approx -31.8$ kcal/mol, if a water molecule serves as a specific acid or $\Delta G° \approx -53.2$ kcal/mol, if an amino acid, namely, histidine, serves as a general acid). Nucleophilic addition of water to cob(III)alamin would generate the oxidized cofactor, H_2OCbl.

A similar mechanism of suicide inactivation has been observed with the R207Q mutant of methylmalonyl-CoA mutase (*8*) and with other AdoCbl-dependent isomerases (*28*, *29*). With the R207Q variant of methylmalonyl-CoA mutase, suicide inactivation is observed in the presence of either isobutyryl-CoA or *n*-butyryl-CoA, and the rate of H_2OCbl formation is $\sim 10^3$-fold slower than that with the Y243A mutant described here (*8*). Inactivation via an internal electron transfer has also been reported for lysine-5,6-aminomutase (*28*), which undergoes inactivation in the presence of D- or L-lysine at a rate that is ~50-fold lower than that observed for Y243A. In the presence of the alternate substrate, *β*-lysine, the rate of inactivation is only ~1.7-fold lower than that reported in this study. Similarly, glutamate mutase in the presence of the substrate analogue 2-methyleneglutarate undergoes suicide inactivation via formation of a Michael adduct between the Ado• and the substrate analogue, followed by an electron transfer from cob(II)alamin (*29*).

Diol dehydratase also experiences suicide inactivation in reactions with substrate analogues (*30*, *31*). The products of inactivation are cob(II)alamin, 5′-deoxyadenosine, and a C_2-product derived from substrate analogues (*27*, *28*) identified as a *cis*-ethanesemidione radical (*32*). The high stability of the glycoaldehyde radical, attributed to the captodative stabilization provided by both the −OH and −CHO groups at the radical center, prevents hydrogen reabstraction by 5′-deoxyadenosine, thus leading to an inactive enzyme (*33*). More interestingly, diol dehydratase also undergoes inactivation in the presence of 5′-deoxy-3′,4′-anhydroadenosine, a cofactor analogue (*30*). Inactivation is postulated to involve an internal electron transfer from cob(II)alamin to the 5′-deoxy-3′,4′-anhydroadenosyl radical, stabilized by allylic delocalization, followed by protonation of the resulting carbanion (*30*).

These examples serve to illustrate the potential susceptibility of the AdoCbl-dependent isomerases to inactivation and the challenge for these enzymes to minimize these reactions.

These suicidal reactions can occur either via a simple oxidation, where molecular oxygen acts as the oxidant, or by internal electron transfer, where commonly a substrate-derived carbanion is transiently formed and rapidly quenched by protonation. These examples also underscore the crucial roles of active site residues in guiding the fate of the radical intermediates and in suppressing suicidal oxidations.

REFERENCES

1. Banerjee, R. (2003) Radical carbon skeleton rearrangements: catalysis by coenzyme B12-dependent mutases, *Chem. Rev. 103*, 2083−2094.
2. Chowdhury, S., and Banerjee, R. (2000) Thermodynamic and kinetic characterization of Co−C bond homolysis catalyzed by coenzyme B_{12}-dependent methylmalonyl-CoA mutase, *Biochemistry 39*, 7998−8006.
3. Thomä, N. H., Meier, T. W., Evans, P. R., and Leadlay, P. F. (1998) Stabilization of radical intermediates by an active site tyrosine residue in methylmalonyl-CoA mutase, *Biochemistry 37*, 14386−14393.
4. Maiti, N., Widjaja, L., and Banerjee, R. (1999) Proton transfer from Histidine244 may facilitate the 1,2 rearrangement reaction in coenzyme B_{12}-dependent methylmalonyl-CoA mutase, *J. Biol. Chem. 274*, 32733−32737.
5. Dybala-Defratyka, A., and Paneth, P. (2001) Theoretical evaluation of the hydrogen kinetic isotope effect on the first step of the methylmalonyl-CoA mutase reaction, *J. Inorg. Biochem. 86*, 681−689.
6. Thoma, N. H., Evans, P. R., and Leadlay, P. F. (2000) Protection of radical intermediates at the active site of adenosylcobalamin-dependent methylmalonyl-CoA mutase, *Biochemistry 39*, 9213−9221.
7. Vlasie, M. D., and Banerjee, R. (2003) Tyrosine 89 accelerates Co-carbon bond homolysis in methylmalonyl-CoA mutase, *J. Am. Chem. Soc. 125*, 5431−5436.
8. Vlasie, M. D., and Banerjee, R. (2004) When a Spectator Turns Killer: Suicidal Electron Transfer from Cobalamin in Methylmalonyl-CoA Mutase, *Biochemistry 43*, 8410−8417.
9. Mancia, F., and Evans, P. (1998) Conformational changes on substrate binding to methylmalonyl CoA mutase and new insights into the free radical mechanism, *Structure 6*, 711−720.
10. Smith, D. M., Golding, B. T., and Radom, L. (1999) The facilitation of enzyme-catalyzed reactions by partial proton transfer: Application to coenzyme B_{12}- dependent methylmalonyl-CoA mutase, *J. Am. Chem. Soc. 121*, 1383−1384.
11. Mancia, F., Smith, G. A., and Evans, P. R. (1999) Crystal structure of substrate complexes of methylmalonyl-CoA mutase, *Biochemistry 38*, 7999−8005.
12. Smith, D. M., Golding, B. T., and Radom, L. (1999) Understanding the mechanism of B_{12}-dependent methylmalonyl-CoA mutase: Partial proton transfer in action, *J. Am. Chem. Soc. 121*, 9388−9399.
13. Dayem, L. C., Carney, J. R., Santi, D. V., Pfeifer, B. A., Khosla, C., and Kealey, J. T. (2002) Metabolic engineering of a methylmalonyl-CoA mutase-epimerase pathway for complex polyketide biosynthesis in *Escherichia coli*, *Biochemistry 41*, 5193−5201.
14. Padmakumar, R., and Banerjee, R. (1995) Evidence from EPR spectroscopy of the participation of radical intermediates in the reaction catalyzed by methylmalonyl-CoA mutase, *J. Biol. Chem. 270*, 9295−9300.
15. Taoka, S., Padmakumar, R., Lai, M.-t., Liu, H.-w., and Banerjee, R. (1994) Inhibition of Human Methylmalonyl-CoA by Various CoA-esters, *J. Biol. Chem. 269*, 31630−31634.
16. Chowdhury, S., and Banerjee, R. (1999) Role of the dimethylbenzimidazole tail in the reaction catalyzed by coenzyme B12-dependent methylmalonyl-CoA mutase, *Biochemistry 38*, 15287−15294.
17. Brooks, A. J., Vlasie, M., Banerjee, R., and Brunold, T. C. (2004) Spectroscopic and computational studies on the adenosylcobalamin-dependent methylmalonyl-CoA mutase: evaluation of enzymatic contributions to Co−C bond activation in the Co3+ ground state, *J. Am. Chem. Soc. 126*, 8167−8180.
18. Pohl, N. L., Hans, M., Lee, H. Y., Kim, Y. S., Cane, D. E., and Khosla, C. (2001) Remarkably broad substrate tolerance of malonyl-CoA synthetase, an enzyme capable of intracellular synthesis of polyketide precursors, *J. Am. Chem. Soc. 123*, 5822−5823.
19. Rupp, H., Rao, K. K., Hall, D. O., and Cammack, R. (1978) Electron spin relaxation of iron-sulphur proteins studied by microwave power saturation, *Biochim. Biophys. Acta 537*, 255−269.
20. Retey, J., Smith, E. H., and Zagalak, B. (1978) Investigation of the Mechanism of the Methylmalonyl-CoA Mutase Reaction with the Substrate Analogue: Ethylmalonyl-CoA, *Eur. J. Biochem. 83*, 437−451.
21. Abend, A., Illich, V., and Retey, J. (1997) Further insights into the mechanism of action of methylmalonyl-CoA mutase by electron paramagnetic resonance studies, *Eur. J. Biochem. 249*, 180−186.
22. Mansoorabadi, S. O., Padmakumar, R., Fazliddinova, N., Vlasie, M., Banerjee, R., and Reed, G. H. (2005) Characterization of a Succinyl-CoA Radical-Cob(II)alamin Spin Triplet Intermediate in the Reaction Catalyzed by Adenosylcobalamin-Dependent Methylmalonyl-CoA Mutase, *Biochemistry 44*, 3153−3158.
23. Zhao, Y., Abend, A., Kunz, M., Such, P., and Retey, J. (1994) Electron paramagnetic resonance studies of the methylmalonyl-CoA mutase reaction: Evidence for radical intermediates using the natural and artificial substrates as well as the competitive inhibitor 3-carboxypropyl-CoA, *Eur. J. Biochem. 225*, 891−896.
24. Carey, F. A., and Sundberg, R. J. (2000) *Advanced Organic Chemistry*, 4th ed., Kluwer Academic/Plenum Publ., New York.
25. Carey, F. A. (2002) *Organic Chemistry*, 5th ed., McGraw-Hill, Boston.
26. Lexa, D., and Saveant, J. M. (1976) Electrochemistry of vitamin B_{12}. I. Role of the base-on/base-off reaction in the oxidoreduction mechanism of the B_{12r}-B_{12s} system, *J. Am. Chem. Soc. 98*, 2652−2658.
27. Jaun, B., Schwarz, J., and Breslow, R. (1980) Determination of the basicities of benzyl, allyl, and *tert*-butylpropargyl anions by anodic oxidation of organolithium compounds, *J. Am. Chem. Soc. 102*, 5741−5748.
28. Tang, K. H., Chang, C. H., and Frey, P. A. (2001) Electron transfer in the substrate-dependent suicide inactivation of lysine 5,6-aminomutase, *Biochemistry 40*, 5190−5199.
29. Huhta, M. S., Ciceri, D., Golding, B. T., and Marsh, E. N. (2002) A novel reaction between adenosylcobalamin and 2-methyleneglutarate catalyzed by glutamate mutase, *Biochemistry 41*, 3200−3206.
30. Magnusson, O. T., and Frey, P. A. (2002) Interactions of diol dehydrase and 3′,4′-anhydroadenosylcobalamin: suicide inactivation by electron transfer, *Biochemistry 41*, 1695−1702.
31. Toraya, T., and Mori, K. (1999) A reactivating factor for coenzyme B12-dependent diol dehydratase, *J. Biol. Chem. 274*, 3372−3377.
32. Abend, A., Bandarian, V., Reed, G. H., and Frey, P. A. (2000) Identification of *cis*-ethanesemidione as the organic radical derived from glycolaldehyde in the suicide inactivation of dioldehydrase and of ethanolamine ammonia-lyase, *Biochemistry 39*, 6250−6257.
33. Sandala, G. M., Smith, D. M., Coote, M. L., and Radom, L. (2004) Suicide inactivation of dioldehydratase by glycolaldehyde and chloroacetaldehyde: an examination of the reaction mechanism, *J. Am. Chem. Soc. 126*, 12206−12207.

BI051742D